Energy & Environmental Science

Learning from existing photovoltaic technologies to identify alternative perovskite module designs

Journal:	*Energy & Environmental Science*
Manuscript ID	EE-PER-06-2020-001923.R1
Article Type:	Perspective
Date Submitted by the Author:	11-Aug-2020
Complete List of Authors:	Werner, Jeremie; University of Colorado at Boulder, Wolf, Eli; NREL; Stanford University, Department of applied physics Boyd, Caleb; Stanford University, Materials Science and Engineering van Hest, Maikel; National Renewable Energy Laboratory, Luther, Joseph; National Renewable Energy Laboratory, Zhu, Kai; National Renewable Energy Laboratory, Chemical and Materials Science Center Berry, Joseph; National Renewable Energy Laboratory (NREL), United States, National Center for Photovoltaics McGehee, Michael; University of Colorado Boulder, Chemical and Biological Engineering

Learning from existing photovoltaic technologies to identify alternative perovskite module designs

Jérémie Werner,[1, 2] Caleb C. Boyd,[2,4] Taylor Moot,[2] Eli J. Wolf,[2,5] Ryan M. France,[2]

Samuel A. Johnson,[3] Maikel F.A.M. van Hest,[2] Joseph M. Luther,[2] Kai Zhu,[2] Joseph

*J. Berry,[2] Michael D. McGehee[1, 2, 3 *]*

[1] Chemical and Biological Engineering, University of Colorado, Boulder, CO 80309, USA

[2] National Renewable Energy Laboratory, 15013 Denver West Parkway, Golden,

CO 80401, USA

[3]Materials Science and Engineering, University of Colorado, Boulder, CO 80309, USA

[4]Materials Science and Engineering, Stanford University, Stanford, CA 94305, USA.

[5]Department of Applied Physics, Stanford University, Stanford, CA 94305, USA.

E-mail: Michael.McGehee@Colorado.edu

Abstract

Perovskite solar cells have now become the most efficient of all multicrystalline thin film photovoltaic technologies, reaching 25.2% in 2019. This outstanding figure of merit has only been achieved on small lab-scale devices, with significantly lower performance when processed on larger more industrially relevant substrate sizes. Perovskite modules, connecting several smaller area cells together, are commonly demonstrated with a superstrate monolithic interconnection method. However, several other module designs exist and remain largely unexplored by the perovskite community. In this work, we review and highlight those alternatives and discuss their advantages and limitations. We propose that a singulated substrate-oriented module design, using metallic substrates, could provide a quicker path to seeing highly efficient, lightweight, and flexible perovskite modules on the market, while mitigating near-term technical risks. As an experimental starting-point towards this design, we demonstrate a substrate-oriented all-perovskite 2-terminal tandem with 18%.

Broader context

Perovskite solar cells have achieved tremendous progress in relatively short period of time, both for their record power conversion efficiency now reaching ~25% and their operational stability, with regular reports of >1000 hours of stable operation. Transferring these achievements from individual small cells in an academic laboratory to large area modules with multiple cells in an industrial production line while reaching commercial competitiveness with other photovoltaic technologies is still a major challenge. High film uniformity over large areas combined with high production yield is required to ensure cost-effective manufacturing. This perspective article presents and discusses the specific hurdles associated with thin-film solar module design. It shines light on several module

designs that have been implemented by other thin-film technologies but have not yet been used for perovskite photovoltaics.

Perovskite solar cells have shown extremely rapid progress in academic lab-scale (<<1 cm^2) device performance, with record efficiencies now at 25.2% and approaching that of c-Si, after just over a decade of research.[1] Unfortunately, the efficiency rapidly decreases with increasing active area, as illustrated in Figure 1. The cell-to-module efficiency gap is also currently still larger than any other photovoltaic technology. The dichotomy of the highest cell efficiency with the largest cell to module efficiency gap must be reconciled as quickly as possible to enable manufacturing and commercialization.[2–4]

This large efficiency gap between small lab-scale devices and large-scale modules can be attributed to multiple factors. First are the difficulties at mitigating the increased resistive losses by subdividing large cells into smaller interconnected subcells. Second is the complexity of up-scaling processing methods from spin coating to industrial processes relevant to production lines and manufacturing, which require large-scale coating, printing or evaporation techniques, e.g. blade coating, slot-die coating or ink-jet printing.[2,5–9] Much of the progress in cell stability and efficiency relies on the absorber composition and therefore on ink formulation, which can be complex to transfer from one deposition technique to another. All the layers of the solar cell need to be coated over large substrates, i.e. >10,000 cm^2, with high uniformity and without pinholes or electronic defects.[4,10] Such large area film uniformity constraints remain highly challenging for thin film photovoltaic technologies like CIGS and particularly for perovskites, where more complex absorber compositions, low thickness variation tolerance and non-wetting solvent systems can increase difficulties with large-scale manufacturing. If solution-processed perovskite solar cells reach a large market, they will be the first solution processed efficient photovoltaic technology to do so.

All the reports showing perovskite modules have so far focused on one unique design: a monolithic series interconnection. Here, we bring attention to other, underexplored, possibilities of fabricating perovskite modules by learning from industrially proven photovoltaic technologies, such as CIGS, CdTe or c-Si. We review the pros and cons of strategies like metal grid connection, singulation, and other aspects of the device configuration and compare them to the classic monolithic series interconnection schemes. We also review the module design implications on stability, especially under reverse bias. Finally, we demonstrate the fabrication of a substrate-oriented all-perovskite 2-terminal tandem with 18% efficiency and discuss future research challenges.

Monolithic interconnection: Thin-film solar cells like CdTe or perovskites are typically built on a transparent conductive oxide (TCO) coated glass substrate. The TCO acts as the front window of the cell and needs to remain transparent, which consequently limits its sheet resistance to ~10 Ω/sq. Increasing the size of the cell in this condition leads to a rapid increase of the resistive losses, limiting

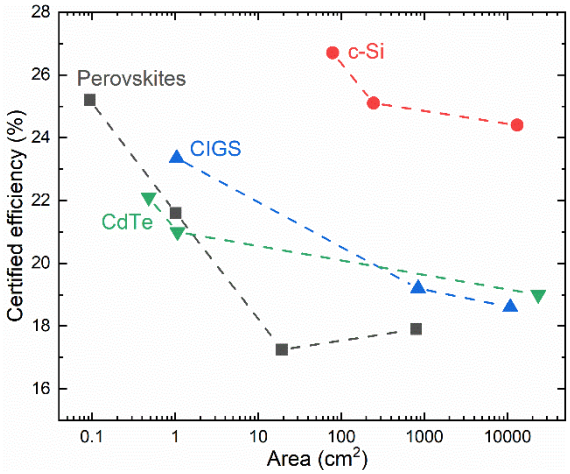

Figure 1: Certified efficiencies as a function of device area for crystalline silicon, CIGS, and CdTe. The record Si module is at 24.4%, 18.6% for CIGS, 19.0% for CdTe and 17.9% for perovskite (with >10x smaller area).

the current flow. Therefore, a large area substrate is usually divided into smaller series-connected subcells, commonly referred to as a monolithic integration (Figure 2a). This design limits the total current that flows through the TCO and therefore minimizes the resistive losses. The subdivision is realized by a scribing approach, either by mechanical scribing or with a laser to ablate the film. The first scribes (often termed "P1") separate the bottom electrode, often a conductive oxide deposited on glass, into many conductive strips generally 0.5-1 cm wide. Then "P2" scribes are applied after the deposition of the selective contacts and absorber layer to open a path to contact the top electrode of one subcell to the bottom electrode of its adjacent subcell. Finally, after deposition of the top electrode, which fills the P2 scribe (also termed a "via"), P3 scribes are necessary to isolate the subcells from one another. Most current thin-film photovoltaic technologies, i.e. CdTe and CIGS, rely on this method to manufacture modules at the industrial level.

The advantages of this method are that it can be fully integrated in a production line and intercalated between the different thin-film deposition steps, allowing for high-throughput without having to handle smaller cells and their subsequent interconnection.

However, this method also has some technical challenges, which are often technology specific and require further development.[4] Scribing with lasers can induce damage to the absorber materials mainly during P2 scribing, e.g. thermal damage in the heat affected zone,[11] film delamination, and spurious residues in the scribe that can lead to shunts. Mechanical scribing may be a potential replacement for lasers in the case of weak adhesion, but it also has its own downsides such as tool wear, difficulties on flexible substrates, and more irregular scribe lines, which increase the module dead area.[12]

The P2 scribe will likely present challenges for device stability due to the direct contact of metal with the absorber material, which can result in chemical reactions, especially for perovskite materials with halide species.[13–16] A P2 scribe will require specific means to passivate and insulate the trench walls without compromising the connection by introducing resistance. Some progress has been made on this front through, for example, careful controls of crystallization dynamics leading to large grains and passivation of interfaces.[13,17–19] This problem will be far more of a challenge in polycrystalline thin-film tandems using perovskite absorbers where more layers need to be scribed and shunting could occur if the metal in the via touches the conductive recombination layer in the center of the tandem.[20] Also considering that a perovskite layer is more volatile and absorbs 355-nm-wavelength laser light more strongly than ITO, the laser parameters might become challenging to adapt to pass through a TCO-perovskite-TCO-perovskite sequence stack, without thermally-induced damage to the absorbers.

The P3 scribe exposes the insides of the device to the environment and therefore requires adequate encapsulation materials that will fill these vias and protect the device absorber from moisture ingress, but without reacting themselves with the absorber and contact materials.[21]

One of the toughest problems for perovskite solar cells is to make large area films with both high structural and electronic uniformity while maintaining high yield in a high-throughput production line. Figure 1 illustrates this challenge, as the largest certified module so far has an area of 800 cm^2 with an efficiency of 17.9%,[22] which is still far from the >10,000 cm^2 achieved by CdTe and CIGS with similar performance.

With this mainstream monolithic integration method, the scribing and interconnection is realized in the production line, usually between the coating steps, but P2 and P3 can in rare cases also be done at the end.[23] Only the final finished and connected module is tested for performance. Therefore, to avoid costly waste of finished large panels, the process must have high yield and thus demands high coating uniformity and reproducibility. This is currently the case for most of the mature CdTe and CIGS module manufacturers. However, anything less than a near unity manufacturing yield in this case can become catastrophic and costly. Thus even the smallest localized defect in one of the stripes, an imperfection in one of the laser scribes, a particle-induced shunt, or a pinhole can significantly lower the performance of an entire 2 m^2 plate thin-film module, affecting both its initial efficiency and long-term stability since defects can lead to increased degradation. Companies like First

Solar have introduced a P4 scribe line in their CdTe modules to mitigate this issue.[24,25] The P4 scribes are performed perpendicularly to the P1, P2 and P3 scribes, separating the long cells into smaller ones. The shorter series connected strings are then connected in parallel. This technique limits the impact of a defect, however, it slightly reduces the active area of the module.

Parallel connection with grid design: A module with parallel connections is made of larger individual subcells, therefore generating higher current, but lower overall voltage than a module using purely series connections. In order to limit the impact of resistive losses, a metal grid is usually needed to improve the charge transport through the TCO-coated glass substrate. Several demonstrations for large area perovskite single cells can already be found in the literature,[26–28] all in superstrate orientation (see section below) with the highest efficiency at 12.1% on a 16 cm^2 area.[27] The challenge in this configuration is to properly design the metal grid pattern to obtain the best compromise between reducing resistive losses of the TCO, which improves FF, and minimizing optical losses through excess shadowing, which limits the losses in current. Moreover, depositing a perovskite cell on top of a metal grid is not straightforward, as the fingers cannot be too thick to avoid solution-processing related non-uniformities and defects, and increasing their width is not desirable as it increases shadowing losses. This thickness problem also rules out some industrial metallization techniques, such as screen-printing. Wires could potentially be embedded into the substrate to maintain a relatively flat surface for the cell deposition; however, this is technically challenging for large scale cells. It is far easier to deposit metals lines on top of a device stack, as we will discuss later for substrate-oriented singulated modules.

Singulated approach: A singulated approach could be used with the same large-area coating techniques but without any intercalated lasering steps. Instead, the full device stack is deposited at once, then the large substrate can be cut down to smaller cells, which can be tested individually. Here, only the dead or poorly performing cells are discarded. The working ones are sorted according to their performance and assembled into series-interconnected strings to form the final module, similar to what is currently done for wafer-based silicon panels. This could lead to the production of modules with different performance ranges, but all working and minimizing material waste. As the best individually tested cells can be assembled in the same module, this method should yield higher module efficiency. Note that the roll- or sheet-to-cell approach just described is not mandatory, it is also easy to imagine a production line with small, pre-cut substrates at the start, similar to a crystalline silicon solar cell production line. This process will be cost-effective only if production speed and throughput can be sufficiently high.

In addition to the crystalline silicon industry and the perovskite/silicon tandems under development, several current and former CIGS companies have used such a singulated approach, including e.g. MiaSolé, SoloPower, or Global Solar, producing the most efficient CIGS large area flexible modules (MiaSolé).[29,30]

Substrate and superstrate orientation: A thin-film solar cell can be made in either *superstrate* orientation (Figure 2a), where it is illuminated through the transparent substrate, i.e. typically FTO or ITO-coated glass, or in *substrate* orientation (Figure 2b) with light coming in from the film side. CdTe modules are typically in superstrate, whereas CIGS are in substrate.[31,32] In superstrate devices, the substrate is both the support for the growth of the device layers and the transparent encapsulant window. For substrate-oriented devices, the substrate is also the support for the films but does not need to be transparent, i.e. metal sheets like stainless steel or metallized polyimide foils are commonly used in CIGS solar cells.

Perovskite solar cells have already been demonstrated in both orientations, thanks to the numerous charge transport materials available and the research work carried out towards perovskite-silicon and perovskite-CIGS tandem solar cells.[33]☐ [33]☐ Only rare studies report on substrate-based single-junction perovskite solar cells, although the concept was already proposed back in 2015 by Troughton *et al.* using metallic titanium substrates.[34] Perovskite mini-modules have so far only been reported in superstrate orientation with a monolithic interconnection design (Figure 2a), to adhere to the mainstream architectures used in lab-scale perovskite solar cells in a vast majority of academic

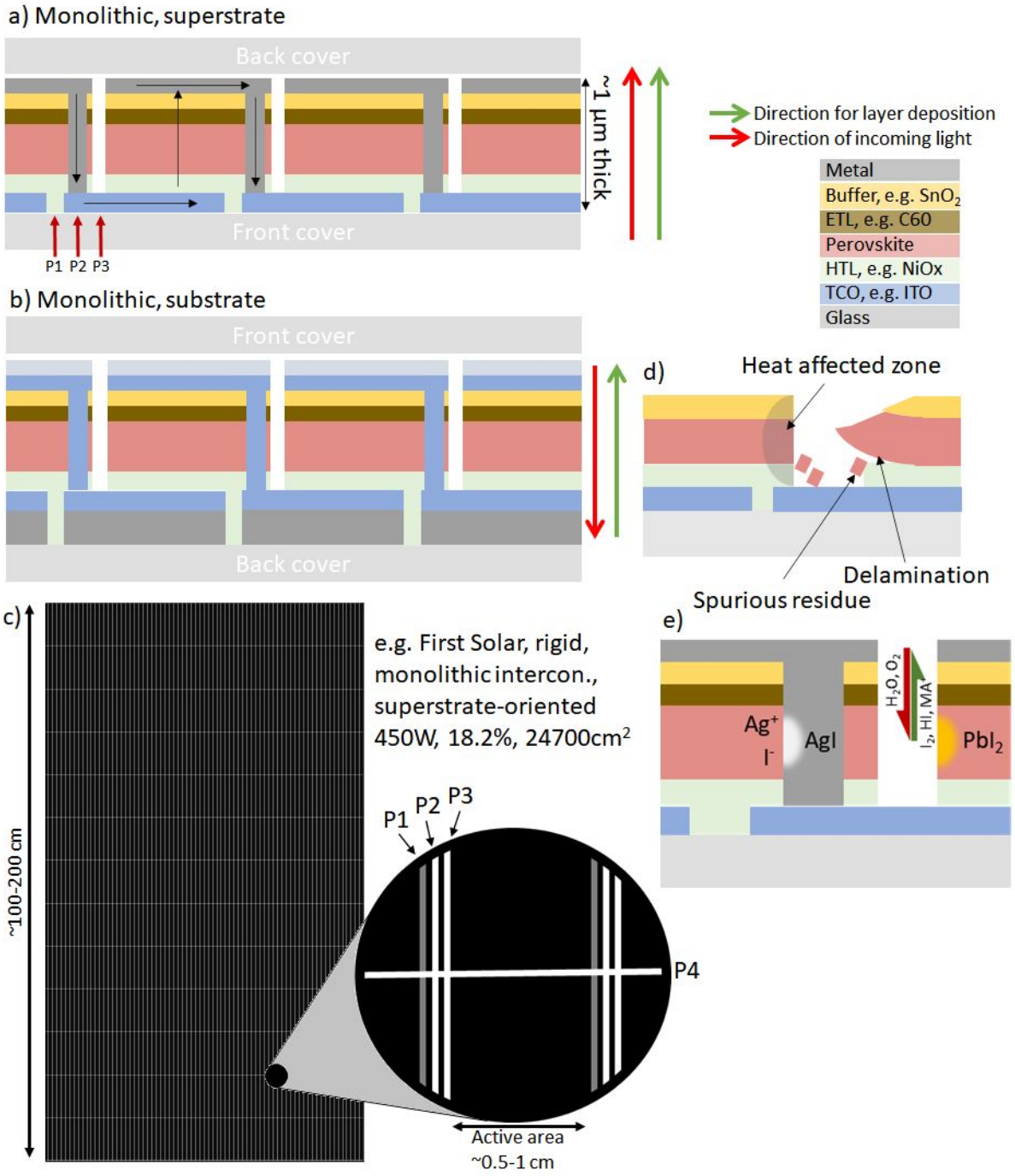

Figure 2: Schematics of monolithically interconnected thin-film modules in a) superstrate or b) substrate orientation. c) Schematic of a full module similar to a First Solar CdTe monolithic module. The magnified area shows closer detail of the P1, P2, P3 and P4 scribe lines. d) Potential damages related to the scribing process. e) Potential degradation mechanisms in P2 and P3 scribe lines.

research groups.

Both superstrate and substrate orientations are compatible with a monolithic interconnection. However, a singulated approach is easier to implement in substrate orientation. Indeed, it is more difficult to fabricate a metal grid on a glass substrate (Figure 3a), without affecting the formation of the absorber layer, than it is to form that absorber on a continuous conductive substrate, i.e. either with a full continuous metal layer under the contact and absorber (Figure 3b) or with the substrate itself being conductive such as steel, aluminum or titanium sheets (Figure 3c). Note that metal foil needs to be relatively smooth (easier to achieve with Al and Ti compared to steel),

cheap and have both high thermal and high electrical conductivity.[35] In particular, a smooth surface finish on the foil is critical to maintain high yield. The surface roughness of Ti foils for example remains challenging for perovskite cells and requires an electropolishing step, which adds cost.[36]

Having a metal substrate also reduces the thickness of the TCO needed to achieve low resistive losses. The front TCO, supported by a metal grid, in substrate-oriented cells will be thinner than the one on the glass of a superstrate-oriented cell, which should be advantageous in terms of costs and parasitic absorption. In standard superstrate monolithic modules, the TCO needs to have high conductivity, i.e. low sheet resistance on the order of ~10 Ω/sq to allow for good charge transport over a ~1-cm-wide cell. This imposes the use of relatively thick TCOs, which can be costly and at the expense of increased parasitic absorption losses.[37] In comparison, a substrate-oriented cell with a transparent electrode deposited last is less sensitive to the TCO conductivity,[38] with typical sheet resistance about 80-100 Ω/sq using a cheaper thinner TCO and a metal grid to compensate for lateral charge transport. A metal grid on the front electrode is easier to make without damaging the underlying layers, and is easier to optimize its geometry,[39] i.e. fingers can be made thicker rather than wider and possibly of different shapes to minimize shading.[40] Such front TCO/metal grids have been extensively researched, are commercially used for silicon solar cells, and further improvements are expected with the development of perovskite/silicon and perovskite/CIGS monolithic tandems, both sharing the same requirements as any substrate-oriented perovskite devices, i.e. low-temperature processing.

In all-perovskite tandems, the device orientation dictates the order in which the two subcells must be deposited.[41] In superstrate orientation, the wide gap subcell is deposited first, then covered with the low gap one. In substrate orientation, however, the low gap cell must be deposited first. Thermal evaporation of the second-deposited subcell in a tandem would also be desirable to avoid solvent-induced damage to the first-deposited subcell; a solvent barrier being one of the most challenging constraints for 2-terminal tandems.

The illumination direction naturally also changes the device optics. Interestingly, a substrate orientation provides the opportunity to introduce a rear-side texture in a tandem,[42] which would be beneficial to enhance light trapping at long wavelengths and ease the constraint on the high absorber thickness required for optimal light absorption in Sn/Pb low bandgap perovskites, which have a relatively low absorption cross-section compared to other perovskites. Ideally, all layers would be deposited conformally on the texture features to obtain optimal anti-reflection and light trapping effects.[43] However, with the commonly used solution-processing methods, a perovskite layer is likely to fill the roughness and planarize it, as observed for perovskite/silicon tandem cells with solution-processed top cells on textured silicon wafers.[44] In a substrate-oriented device, the long wavelength light trapping effect would, however, remain effective for the low bandgap subcell, which would not necessarily be the case in a superstrate configuration. Examples of texturization in the literature are numerous, either with directly textured substrates,[43,45,46] textured oxides,[47,48] or descriptions of the benefits for photoluminescence enhancement.[49]

Interconnections for substrate-oriented singulated modules: A metal grid is needed on the front electrode for charge collection, which can be deposited by standard methods like thermal evaporation, screen printing, or inkjet printing. Thermal evaporation is however usually not suitable for industrial cells, due to higher usage of Ag to produce thick (>500nm) but narrow lines, in order to reach <1 Ω/cm line resistance with increasing shadow losses. Because of the need for shadow masks defining the grid lines during thermal evaporation, a large fraction of the evaporated metal is wasted. Screen printing is therefore usually preferred, especially by the silicon industry, whereas ink-jet printing can be used for CIGS.[23] Both screen-printing and ink-jet printing have also typically lower capital expenses and allow higher production throughput compared to thermal evaporation for the metallization. Screen-printing of a Ag grid has already been demonstrated for perovskite/silicon 2-terminal tandems, with curing in air at 130°C for 10min.[50] Currently, this low temperature is necessary to limit the thermal degradation of the perovskite subcell, even if higher curing temperatures would help to further reduce the line resistance.

The connection between the individual subcells can be made either through a shingling process (Figure 3d) or with wires (Figure 3e&f). In a shingled module, the cells are processed on a conductive substrate, then the connection occurs by overlapping edges of adjacent cells, to contact the bottom electrode of one cell to the top of its neighbor.[31,32,51] An electrically conductive adhesive is usually required to electrically bond the two cells together. This method eliminates all need for wires or ribbons, as well as all dead space in the module. However, it relies on printed grid lines and busbars, which represent significant Ag usage and associated cost. A wire-based strategy is therefore often preferred by the industry, with several examples of innovative solutions, e.g. REC with the SmartWire technology of Meyer Burger,[52,53] UltraWire by Miasolé (Figure 3e),[54] and tiling ribbon from Jinko Solar.[55] Those wires, typically made of copper, are incorporated into a polymer foil and coated with a low-melting point conductive alloy.[56] This alloy melts and makes the solder contact with the printed metallization lines on the cell during module lamination. This requires then lower temperatures, ~140-160°C, as compared to ~200°C for standard ribbon soldering, therefore reducing the thermal stress and potential heat-induced cell degradation. Other advantages of wires over ribbons are optics, with ~25% lower shadowing losses thanks to the rounded geometry of the wires, and cost, as the Ag usage is reduced by ~85%.[52]

We should note that the particular, and rare, case of the metal wrap-through connection technique was used for Nanosolar's thin-film CIGS solar cells.[35] Here, instead of driving the electrical charges laterally in the front metal grid to the external circuit, holes are pierced through the entire cell and substrate, and metallized to direct the charges to a metal sheet contact at the back of the device.[57] These metallized holes bring, however, similar stability concerns as discussed for the P2 scribe line in a standard monolithic module with metal-perovskite interactions.

Reverse bias mitigation by module design: Partial shading is a problem that does not arise naturally in the lab when testing individual solar cells but is commonplace in the field. There are many different situations that can cause one or many cells to be shaded. In the residential space, shadows can be cast onto solar cells by nearby telephone poles, trees, chimneys, and other houses. Even in utility scale installations, with no objects nearby, the top of one row of solar cells can sometimes cast a shadow onto the bottom part of the next row of modules behind at sunrise and sunset. In all cases, partial shading of cells can occur during cloud coverage variation or through soiling originating either from animals (e.g. excrements of pigeons or seagulls, shadow of a human[58] walking by) or weather (e.g. sand, leaves, snow).

Partial or total shading of cells in a string can cause the shaded cells to be forced into reverse bias.[25] When this reverse bias becomes larger than the shaded cell's breakdown voltage, it conducts current, and therefore dissipates power through Joule heating. The power dissipates through low resistance pathways, which can be existing defects, leading to the formation of hot spots. There, the temperature can rise >100°C and cause irreversible damage to the cell or its encapsulation. Since shading is unavoidable in any type of photovoltaic panel, measures need to be taken to ensure reverse bias exposures will not irremediably damage the modules.[25,59,60]

A substrate-oriented module with a thermally conductive substrate, e.g. a metal foil, could help to distribute the generated heat and spread it more uniformly over the entire cell, reducing the maximum hot spot temperature. Reverse bias degradation remains scarcely studied for perovskite solar cells. The rare studies report on element migration (e.g. iodine),[61] hot spots,[62] metal ingress and shunting, and electrochemical degradation.[63] Also, the reverse breakdown voltage is dependent on the choice of charge transport layer materials and ranges typically from -1 to -4V.[63] This provides a design tool at the cell level to limit the maximum power that the shaded cell has to dissipate by reducing the breakdown voltage, i.e. each cell becomes effectively its own bypass diode. For example, in CIGS cells, reducing the absorber thickness was shown to reduce the breakdown voltage.[25]

Little to no investigation has been carried out with perovskite solar cells to evaluate module designs to lower the reverse bias risks.[62] Moreover, a singulated approach offers more options for module topology, cells arrangement, and bypass diode configuration, when compared to a monolithic module. When many cells are electronically connected to form a module, different topologies[64] can

be selected to adjust nominal operating voltages and currents, by interconnecting cells in parallel groups and then connecting those groups in series. This strategy should reduce the voltage across the shaded cells, but at the expense of increased series resistance losses as well as wiring cost and

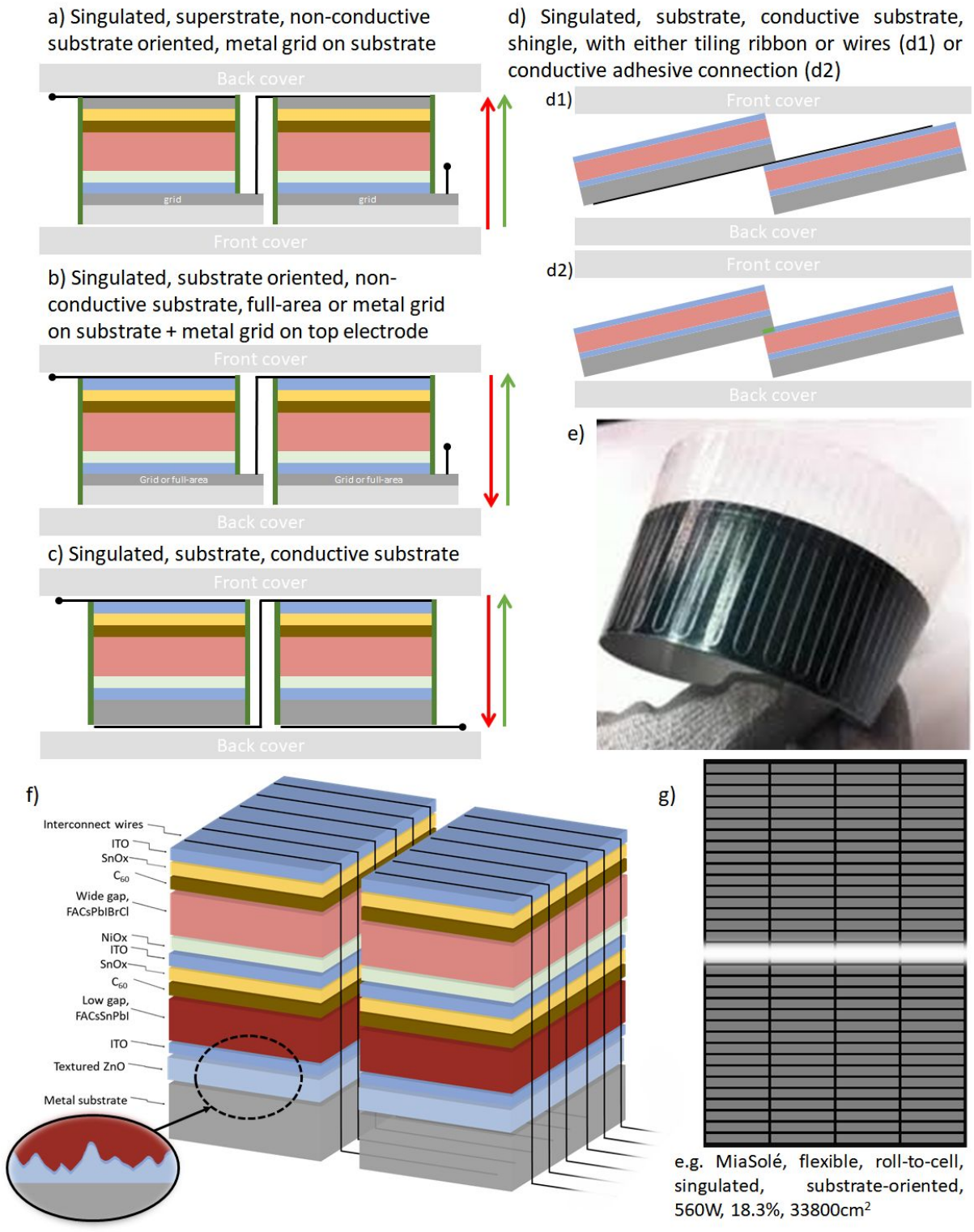

Figure 3: Singulated solar cells – cross-section schematic of a singulated thin-film module in a) superstrate and b-c) substrate orientation, using in c) a metallic substrate and in a&b possibly a metal grid on the supporting substrate (i.e. glass) to reduce series resistance in the TCO; d) illustration of a shingled module with singulated substrate-oriented cells on metallic substrates; e) Examples of MiaSolé UltraWire interconnection technology on a flexible stainless steel CIGS cell;[54] f) Our proposed perovskite tandem cell structure which at the module level could look like the module in g). Green arrow denotes deposition direction and red arrow denotes illumination direction.

complexity. Determining the best solution and/or combination of solutions to overcome partial shading induced reverse bias will be important.

Alternative perovskite module design: Table 1 is summarizing the discussed advantages and disadvantages of the standard superstrate-oriented monolithically interconnected module and the proposed alternative design with substrate-oriented singulation. Figure 3g shows a visual example of a module using a singulated substrate-oriented approach, as used e.g. with CIGS cells by MiaSolé.[54] A perovskite module could follow a similar design, which would be broadly applicable and could facilitate near term large-scale manufacturing. We can now summarize the features of this proposed perovskite module design (Figure 3f). The module production line would be similar to other standard thin-film solar cells, including the preferred large area coating systems, and could start with large rigid substrates or flexible rolls. A surface texturing coating (e.g. LPCVD ZnO) or treatment (e.g. etching, scribing) could first be applied to these substrates. ZnO is a strong candidate as it was already ramped up to industrial scale for thin film silicon solar cells, with proven low cost and reliable processes.[65] Instabilities with perovskite materials should however be considered and will likely require a barrier layer.[66] Then, all the layers of the devices would be coated in sequence. The large substrate would then be cut down to the final smaller cells. Those could be tested individually and sorted by performance, before being assembled accordingly into the final module. The interconnection scheme would ideally adopt industrially available technologies, such as the UltraWire or SmartWire from the CIGS or c-Si industries. This concept could help to accelerate the technological transfer from research labs to industry, by avoiding many pitfalls of standard up-scaling processes, and potentially yield modules with higher efficiencies on a shorter time scale.

Some challenges: Obviously, this type of module design does not come without challenges. Deposition of a perovskite cell on a metal substrate requires some precautions to avoid undesired reactions between the metal and the halide species of the absorber. The substrate needs to be chosen carefully, taking into consideration thermal constraints of the process, no outgassing during fabrication or operation, no reaction with the contact or absorber layers, regular roughness (i.e. no spikes, grooves or cavities) which is not trivial and might require either a polishing step or the application of a planarizing coating, appropriate thermal and electrical conductivity, lightweight, possibly flexible, and certainly low cost. Its thermal expansion mismatch with the perovskite absorber should also be minimized to avoid stress accumulation during fabrication,[67] and in this context, a metal substrate with higher thermal expansion coefficient than glass could be advantageous. Deposition of a Sn/Pb perovskite on a textured substrate has yet to be demonstrated, especially on a textured ZnO, which will require a barrier layer (likely a thin ITO layer can be sufficient) to avoid reactions with the perovskite layer.[66,68] Metal foils can also be directly textured for example by anodization.[69,70] However, a significant initial challenge to building an all-perovskite tandem in this design is to invert the subcell growth order, i.e. the low gap cell has to be deposited first, then covered with the wide gap cell. Therefore, the Sn/Pb perovskite cell must show sufficiently high thermal stability to sustain the thermal constraint of the deposition of the wide gap subcell. Sn/Pb perovskites often tend to have larger surface roughness,[71] as compared to their wide gap pure Pb counterparts, due to their higher film thickness. This can influence the solvent barrier properties of the recombination junction, which might need to be reengineered accordingly.

Table 1: Summary of pros & cons for the standard superstrate configuration with monolithic integration and the proposed substrate configuration with singulation.

Monolithic, superstrate		**Singulated, substrate**	
Pros	Cons	Pros	Cons
• In-line process, all integrated, high-throughput • Translatable experience from CdTe, a-Si & CIGS industries • Device structure closer to the mainstream perovskite architectures developed in most laboratories • For tandems, wide-gap perovskite cells are now more thermally stable, therefore better suited as the underlying subcell	• High uniformity required on large area, and high yield in production line • PCE tested only at final stage on full module, potential issues with yield • Only transparent substrates • Scribing-induced damages, e.g. in P2 lines • TCO resistive losses • Reverse bias degradation difficult to mitigate	• Smaller cell, lower technical constraint on large area uniformity • Individual cells can be tested and sorted before assembly in final module • Similarity with mainstream c-Si production line, similar requirements for front electrode & metallization and module assembly • Can use any type of substrates, including metallic & opaque ones • Use of metal substrates can lower the requirement on high quality TCO, with lower resistive losses • No scribing, so no metal-absorber direct contact • Shared structure and thus development with other perovskite-based multijunction cells • Facilitates introduction of rear-side texture which could provide higher IR response in tandems • Thermal dissipation in metal substrates to reduce effect of hot spots • Offers variable options for module topology and bypass diodes arrangements	• Must handle small samples for module assembly, which might impact throughput and therefore manufacturing cost • Limited know-how and success stories in thin-film solar industry • Front electrode requires transparent TCO & metal grid deposited at low temperature/low damage • For tandems, need high thermal stability in narrow bandgap perovskite subcell • Metal foil surface roughness

Substrate-oriented 2-terminal tandem demonstration: As a first step towards the proposed perovskite module design, Figure 4 shows a first proof-of-concept for a substrate-oriented all-perovskite 2-terminal tandem. The tandem was made with a 1.25 eV band gap $FA_{0.75}Cs_{0.25}Sn_{0.5}Pb_{0.5}I_3$ perovskite subcell formed with our recently published gas quenching method.[71] The recombination junction comprises of a 15 nm-thick SnO_x layer grown by atomic layer deposition, a 10 nm-thick sputtered ITO layer and a sputtered 20 nm-thick NiO_x layer. The combination of these three compact layers creates a strong solvent barrier, even on rough films such as the Sn/Pb perovskites. The wide gap cell was made of a 1.74 eV band gap $FA_{0.7}Cs_{0.25}MA_{0.05}Pb(I_{0.7}Br_{0.25}Cl_{0.05})_3$ perovskite with 6% molar excess FAI in solution to improve the voltage on NiO_x.[72]

This first substrate-oriented perovskite tandem had ~18% power conversion efficiency, with a large room for improvement, especially in FF. This device structure will however now share, in addition to its configuration, many optimization paths with its fellow perovskite-based tandems, perovskite/silicon and perovskite/CIGS. This includes, among others, tuning the bandgap and thickness of the wide gap cell to ensure current matching conditions, reducing parasitic absorption losses with optimized transparent electrodes and recombination junctions, reducing the voltage deficit of the wide gap cell, reducing interfacial resistance losses, increasing the stability of both subcells (particularly the thermal stability of the Sn/Pb perovskite device), growing Sn/Pb perovskite cells on textured surfaces, and avoiding metal diffusion and reactions from the metal substrate and the front grid with the cell elements.[73]

Remaining technical and economical questions: We believe that there are several still open important questions that require a particular attention from the community to identify which architecture will ultimately be superior (see Table 1 as well):

(1) What is the current uniformity of perovskite solar cells using established deposition methods (i.e. slot-die coating, vapor deposition)? What are the number of defects, e.g. pinholes, per square meter?

(2) How much would it cost to throw away a certain percentage of perovskite modules at the end of the production line? A thin film solar company such as First Solar is certainly well positioned to know how this impacts production costs. The information is however not publicly available.

(3) How much cost does it add to assemble smaller, higher-yield singulated substrates into a module as compared to scribing monolithic interconnects? Here, a company such as MiaSolé would have some insights, but again not much is publicly available.

In conclusion, we proposed considerations for alternative research directions for the fabrication of perovskite solar modules by looking at what other thin-film solar cell industries have implemented. We discussed the adoption of a substrate configuration and the use of singulation in module design, which could be appropriate for the near-term development of this technology where technical hurdles of up-scaling and film uniformity remain problematic. Finally, we demonstrated a substrate-oriented all-perovskite 2-terminal tandem with 18% efficiency and discussed its remaining

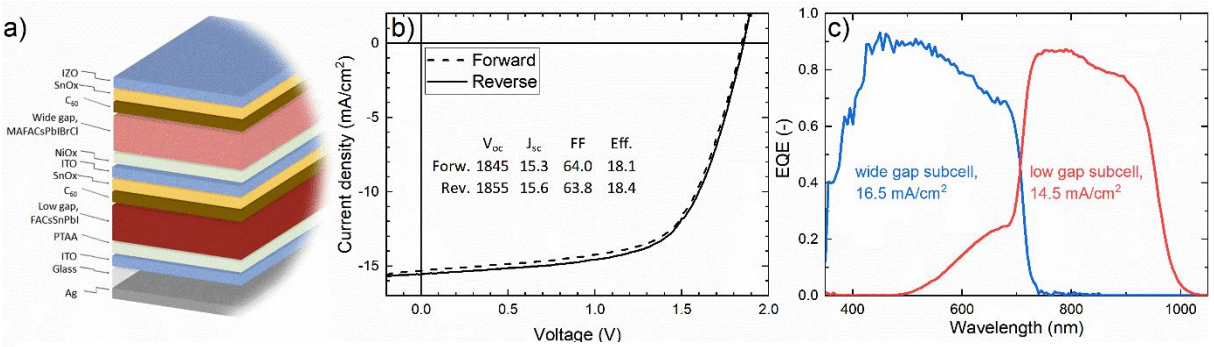

Figure 4: Experimental demonstration of a substrate-oriented all-perovskite 2-terminal tandem. a) Device schematic. b) Current density-voltage curves of the tandem in forward (dashed line) and reverse (solid) scan directions. c) External quantum efficiency measurements of the tandem with the wide bandgap cell (blue) and the narrow bandgap cell (red).

challenges. Although in the current fast paced research field and competitive photovoltaic market it is difficult to predict near and long-term industrial successes, adopting this alternative module design could make perovskite modules move faster up the learning curve and ease the path to high efficiency, lightweight, and flexible modules.

Methods

All perovskite precursor chemicals were used as received and stored inside a nitrogen glovebox. All steps were conducted in a nitrogen glovebox. Perovskite precursor solutions were prepared by dissolving formamidinium iodide (Greatcell), cesium iodide (Sigma Aldrich, 99.999%, lot#MKBK6132V), tin (II) iodide (Sigma Aldrich, 99.999% beads in N_2-sealed ampoules), tin fluoride (Aldrich, 99%, lot#MKCK3960), and lead (II) iodide (Alfa Aesar, lot#Z13E032), in a mixture comprising N,N dimethylformamide (DMF, Sigma Aldrich) and dimethylsulfoxide (DMSO, Sigma Aldrich), in a 4:1 volume ratio. The concentration was 2M and nominal composition was $FA_{0.75}Cs_{0.25}Sn_{0.5}Pb_{0.5}I_3$. The tin fluoride was weighted at 10 mol% of the SnI_2 content. The solution was left stirring at room temperature overnight to ensure complete dissolution of the precursors, then filtered just before spinning, using PTFE filters with pore size of 0.2 µm. Poly[bis(4-phenyl)(2,4,6-trimethylphenyl)amine] (PTAA, Solaris Chem Inc., Mw. 20-75kDa, SOL2426M) solution was prepared in a N_2-filled glovebox, with concentration of 1mg/ml in chlorobenzene, stirred overnight.

ITO-coated glass substrates (Colorado Concept Coatings, 2.5 cm x 2.5 cm x 1 mm, 15-20 Ω/sq) were cleaned by successive sonication in baths of acetone and isopropanol, followed by 15 minutes of UV-ozone exposure right before use. The PTAA was spun at 6000 rpm for 30 seconds, in a dynamic drip, and annealed for 10 minutes at 100°C. 35 µl of perovskite precursor solution was spread over the substrate with a pipette tip, and spun at 5000 rpm for 40 seconds. A nitrogen gun was then positioned on top of the spinning substrate at about 5 cm away and started after 10-12 seconds into the spin cycle. The gas flow was sustained until the film had turned dark brown, followed by annealing at 120°C for 10 minutes. 30 nm of C_{60} was then thermally evaporated, followed by ALD deposition of SnO_x, and ITO and NiO_x sputtering. Atomic layer deposition of SnO_x was achieved using a Beneq TFS200 ALD system; 121 cycles of hot sourced (55°C) (tetrakis)dimethyl amido tin (IV) (Sterm) and water, with a growth rate of 1.24 A/cycle; reactor wall temperature of 90°C, pressure of 3 mbar of nitrogen carrier gas. The devices were loaded and unloaded in ambient air, then immediately moved to inert atmosphere. ITO was sputtered in a Denton Explorer 14 sputter tool from a 99.99% pure 2” diameter In2O3/SnO2 90/10 wt% target from Kurt J. Lesker at 30W in an air mixture of 0.04% O2 and 99.6% Ar at 4 mTorr at room temperature. NiO_x was RF sputtered in a Denton Explorer 14 sputter tool from a 99.9% pure 2” diameter NiO target from Kurt J. Lesker at 60W in pure Ar at 16.5 mTorr at room temperature. The wide gap subcell (Eg~1.74eV) was then deposited as previously reported in ref.[72]

Solar cells were tested for quantum efficiency using a calibrated, custom-built tool by scanning chopped, monochromated light from 350 to 1050 nm while light biasing with continuous LEDs. The top cell was tested while flooding the bottom cell with 940 nm light and the bottom cell was tested while flooding the top cell with 470 nm light. No impacts of luminescent coupling on the quantum efficiency were observed. Illuminated JV data was acquired on an adjustable continuous simulator that combines light from a Xe bulb with variable-intensity LEDs. The spectrum was adjusted to the AM1.5g global spectrum by using the measured EQE along with spectral mismatch factors to determine the subcell photocurrents,[74] and the spectrum was measured using calibrated reference cells with bandgaps of 1.8, 1.4, and 1.0-eV, leading to errors in photocurrent ratio from the global spectrum of less than 1%. Cells were tested in a 4-probe using a shadow mask with aperture area 0.06 cm^2, and scan rate of 0.1 V/s. Note that the difference in the J_{sc} from the integrated EQE and the measured J_{sc} from JV scans is due to differences in measurement condition and small measurement errors.[75] We use the EQE to accurately set up the AM1.5 global spectrum for JV measurement.[74]

Acknowledgements

This material is based upon work supported by the U.S. Department of Energy's Office of Energy Efficiency and Renewable Energy (EERE) under Solar Energy Technologies Office (SETO) Agreement Number DE-EE0008551 and partially by the Office of Naval Research under award number N00014-17-1-2212. Work at the National Renewable Energy Laboratory was supported by the US DOE under Contract Number DE-AC36-08GO23808 and the Operational Energy Capability Improvement Fund of the Department of Defense. C.C.B. acknowledges support from the National Science Foundation Graduate Research Fellowship under Grant No. DGE-1656518. The authors would like to thank Lorelle Mansfield for discussions regarding CIGS device manufacturing.

Authors contributions

J.W. and M.D.M. designed the project. J.W. drafted most of the manuscript, prepared all manuscript figures, and developed the tandem layer stack and process flow. C.C.B. and T.M. fabricated the tandem devices and contributed to the design of the manuscript figures. S.A.J. carried out the ALD depositions. E.J.W. contributed on the reverse bias section. R.M.F. carried out the electrical characterization of the tandem cells. M.F.A.M.v.H., J.M.L., K.Z., J.J.B. and M.D.M. provided important conceptual insights about thin-film solar module manufacturing. All co-authors contributed to the manuscript writing and discussions. M.D.M. supervised the project.

References

1. NREL. Best Research-Cell Efficiency Chart. https://www.nrel.gov/pv/cell-efficiency.html (2020).
2. Qiu, L., He, S., Ono, L. K., Liu, S. & Qi, Y. Scalable Fabrication of Metal Halide Perovskite Solar Cells and Modules. *ACS Energy Letters* **4**, 2147–2167 (2019).
3. Hu, Y. *et al.* Standardizing Perovskite Solar Modules beyond Cells. *Joule* **3**, 2076–2085 (2019).
4. Park, N. & Zhu, K. Scalable fabrication and coating methods for perovskite solar cells and solar modules. *Nature Reviews Materials* **5**, 333-350 (2020).
5. Li, H. *et al.* Recent progress towards roll-to-roll manufacturing of perovskite solar cells using slot-die processing. *Flexible and Printed Electronics* **5**, 014006 (2020).
6. Patidar, R., Burkitt, D., Hooper, K., Richards, D. & Watson, T. Slot-die coating of perovskite solar cells: An overview. *Materials Today Communications* **22**, 100808 (2020).
7. Li, Z. *et al.* Scalable fabrication of perovskite solar cells. *Nature Reviews Materials* **3**, 1–20 (2018).
8. Dai, X. *et al.* Scalable Fabrication of Efficient Perovskite Solar Modules on Flexible Glass Substrates. *Advanced Energy Materials* **10**, 1903108 (2020).
9. Ding, J. *et al.* Fully Air-Bladed High-Efficiency Perovskite Photovoltaics. *Joule* **3**, 402–416 (2019).
10. Kim, D. H., Whitaker, J. B., Li, Z., van Hest, M. F. A. M. & Zhu, K. Outlook and Challenges of Perovskite Solar Cells toward Terawatt-Scale Photovoltaic Module Technology. *Joule* **2**, 1437–1451 (2018).
11. Kosasih, F. U., Rakocevic, L., Aernouts, T., Poortmans, J. & Ducati, C. Electron Microscopy Characterization of P3 Lines and Laser Scribing-Induced Perovskite Decomposition in Perovskite Solar Modules. *ACS Applied Materials and Interfaces* **11**, 45646–45655 (2019).
12. Murison, R. *et al.* CIGS P1, P2, and P3 laser scribing with an innovative fiber laser. *Conference Record of the IEEE Photovoltaic Specialists Conference* 179–184 (2010) doi:10.1109/PVSC.2010.5614550.
13. Bi, E. *et al.* Efficient Perovskite Solar Cell Modules with High Stability Enabled by Iodide Diffusion Barriers. *Joule* **3**, 2748–2760 (2019).
14. Raiford, J. A. *et al.* Enhanced Nucleation of Atomic Layer Deposited Contacts Improves Operational Stability of Perovskite Solar Cells in Air. *Advanced Energy Materials* **9**, 1902353 (2019).

15. Zhao, J. *et al.* Is Cu a stable electrode material in hybrid perovskite solar cells for a 30-year lifetime? *Energy and Environmental Science* **9**, 3650–3656 (2016).
16. Domanski, K. *et al.* Not All That Glitters Is Gold: Metal-Migration-Induced Degradation in Perovskite Solar Cells. *ACS Nano* **10**, 6306–6314 (2016).
17. Liu, Z. *et al.* Gas-solid reaction based over one-micrometer thick stable perovskite films for efficient solar cells and modules. *Nature Communications* **9**, 1–11 (2018).
18. Liu, Z. *et al.* A holistic approach to interface stabilization for efficient perovskite solar modules with over 2,000-hour operational stability. *Nature Energy* 1–9 (2020) doi:10.1038/s41560-020-0653-2.
19. Jiang, Y. *et al.* Negligible-Pb-Waste and Upscalable Perovskite Deposition Technology for High-Operational-Stability Perovskite Solar Modules. *Advanced Energy Materials* **9**, 1803047 (2019).
20. Bush, K. A. Stable perovskite module interconnects (US 10644179B1).
21. Cheacharoen, R. *et al.* Encapsulating perovskite solar cells to withstand damp heat and thermal cycling. *Sustainable Energy and Fuels* **2**, 2398–2406 (2018).
22. NREL. Champion Photovoltaic Module Efficiency Chart. https://www.nrel.gov/pv/module-efficiency.html (2020).
23. Fields, J. D. *et al.* Printed interconnects for photovoltaic modules. *Solar Energy Materials and Solar Cells* **159**, 536–545 (2017).
24. FirstSolar. *First Solar Series 6 ™ 420-450 Watts*. http://www.firstsolar.com/en/Modules/Series-6 (2020).
25. Silverman, T. J., Mansfield, L., Repins, I. & Kurtz, S. Damage in monolithic thin-film photovoltaic modules due to partial shade. *2017 IEEE 44th Photovoltaic Specialist Conference, PVSC 2017* **6**, 1–6 (2017).
26. Hambsch, M., Lin, Q., Armin, A., Burn, P. L. & Meredith, P. Efficient, monolithic large area organohalide perovskite solar cells. *Journal of Materials Chemistry A* **4**, 13830–13836 (2016).
27. Kim, J. *et al.* Overcoming the Challenges of Large-Area High-Efficiency Perovskite Solar Cells. *ACS Energy Letters* **2**, 1978–1984 (2017).
28. Wilkinson, B., Chang, N. L., Green, M. A. & Ho-Baillie, A. W. Y. Scaling limits to large area perovskite solar cell efficiency. *Progress in Photovoltaics: Research and Applications* **26**, 659–674 (2018).
29. MiaSolé flexible module record. http://miasole.com/miasole-breaks-world-record-again-large-area-flexible-photovoltaic-module-with-18-64-efficiency/.
30. Green, M. A. *et al.* Solar cell efficiency tables (Version 55). *Progress in Photovoltaics: Research and Applications* **28**, 3–15 (2020).
31. Yan, F., Metacarpa, D. J., Sundaramoorthy, R., Fobare, D. & Haldar, P. Evaluation of CIGS cell interconnection methods. *Conference Record of the IEEE Photovoltaic Specialists Conference* 2064–2067 (2013) doi:10.1109/PVSC.2013.6744879.
32. Bermudez, V. & Perez-Rodriguez, A. Understanding the cell-to-module efficiency gap in Cu(In,Ga)(S,Se)2 photovoltaics scale-up. *Nature Energy* **3**, 466–475 (2018).
33. Fu, F. *et al.* High-efficiency inverted semi-transparent planar perovskite solar cells in substrate configuration. *Nature Energy* **2**, 16190 (2016).
34. Troughton, J. *et al.* Highly efficient, flexible, indium-free perovskite solar cells employing metallic substrates. *Journal of Materials Chemistry A* **3**, 9141–9145 (2015).
35. *Ultra-Low-Cost Solar Electricity Cells: An Overview of Nanosolar' s Cell Technology Platform*. (2009).
36. Lee, M., Jo, Y., Kim, D. S., Jeong, H. Y. & Jun, Y. Efficient, durable and flexible perovskite photovoltaic devices with Ag-embedded ITO as the top electrode on a metal substrate. *Journal of Materials Chemistry A* **3**, 14592–14597 (2015).
37. Morales-masis, M., de Wolf, S., Woods-robinson, R., Ager, J. W. & Ballif, C. Transparent Electrodes for Efficient Optoelectronics. *Advanced Electronic Materials* **3**, 1600529 (2017).

38. Rowell, M. W. & McGehee, M. D. Transparent electrode requirements for thin film solar cell modules. *Energy and Environmental Science* **4**, 131–134 (2011).
39. van Deelen, J., Klerk, L. & Barink, M. Optimized grid design for thin film solar panels. *Solar Energy* **107**, 135–144 (2014).
40. Saive, R. *et al.* Effectively Transparent Front Contacts for Optoelectronic Devices. *Advanced Optical Materials* **4**, 1470–1474 (2016).
41. Moot, T. *et al.* Choose your own adventure: fabrication of monolithic all-perovskite tandem photovoltaics. *Advanced Materials* **in press**, (2020).
42. Zhu, L. *et al.* Modeling and design for low-cost multijunction solar cell via light-trapping rear texture technique: Applied in InGaP/GaAs/InGaAs triple junction. *Progress in Photovoltaics: Research and Applications* pip.3217 (2019) doi:10.1002/pip.3217.
43. Sahli, F. *et al.* Fully textured monolithic perovskite/silicon tandem solar cells with 25.2% power conversion efficiency. *Nature Materials* **17**, 820-826 (2018).
44. Chen, B. *et al.* Blade-Coated Perovskites on Textured Silicon for 26%-Efficient Monolithic Perovskite/Silicon Tandem Solar Cells. *Joule* **4**, 850–864 (2020).
45. Cao, S. *et al.* Light Propagation in Flexible Thin-film Amorphous Silicon Solar Cells with Nanotextured Metal Back Reflectors. *ACS Applied Materials & Interfaces* **12**, 26184-26192 (2020).
46. Tavakoli, M. M. *et al.* Efficient, flexible and mechanically robust perovskite solar cells on inverted nanocone plastic substrates. *Nanoscale* **8**, 4276–4283 (2016).
47. Nicolay, S., Despeisse, M., Haug, F. J. & Ballif, C. Control of LPCVD ZnO growth modes for improved light trapping in thin film silicon solar cells. *Solar Energy Materials and Solar Cells* **95**, 1031–1034 (2011).
48. Haug, F.-J. & Ballif, C. Light management in thin film solar cells. *Energy & Environmental Science* **8**, 824–837 (2010).
49. Richter, J. M. *et al.* Enhancing photoluminescence yields in lead halide perovskites by photon recycling and light out-coupling. *Nature Communications* **7**, (2016).
50. Kamino, B. A. *et al.* Low-Temperature Screen-Printed Metallization for the Scale-Up of Two-Terminal Perovskite-Silicon Tandems. *ACS Applied Energy Materials* **2**, 3815–3821 (2019).
51. Oh, W. *et al.* Design of a solar cell electrode for a shingled photovoltaic module application. *Applied Surface Science* **510**, 145420 (2020).
52. Söderströma, T., Papetb, P., Yao, Y. & Ufheil, J. Smartwire Connection Technology - Meyer Burger. *Smartwire Connection Technology* 12 (2014).
53. REC. *REC Alpha Series*. https://usa.recgroup.com/alpha?parent=1480&type=product.
54. MiaSolé. *MiaSolé Flex Series - 03W 2.6Meter - Datasheet*. http://miasole.com/products/.
55. JinkoSolar. *Tiger N-Type Mono-facial Datasheet*. https://www.jinkosolar.com/en.
56. Faes, A. *et al.* Smartwire Solar Cell Interconnection Technology. *PVSEC 29th* 2555–2561 (2014).
57. Lochun, D., Sheats, J. R. & Miller, G. A. High-efficiency solar cell with insulated vias. (2007).
58. Silverman, T. J. & Repins, I. Partial Shade Endurance Testing for Monolithic Photovoltaic Modules. in *2018 IEEE 7th World Conference on Photovoltaic Energy Conversion* 3932–3937 (2018). doi:10.1109/PVSC.2018.8547832.
59. Silverman, T. J. *et al.* Thermal and electrical effects of partial shade in monolithic thin-film photovoltaic modules. *2015 IEEE 42nd Photovoltaic Specialist Conference, PVSC 2015* **5**, 1742–1747 (2015).
60. Ahsan, S., Niazi, K. A. K., Khan, H. A. & Yang, Y. Hotspots and performance evaluation of crystalline-silicon and thin-film photovoltaic modules. *Microelectronics Reliability* **88–90**, 1014–1018 (2018).
61. Razera, R. A. Z. *et al.* Instability of p-i-n perovskite solar cells under reverse bias. *Journal of Materials Chemistry A* **8**, 242–250 (2019).
62. Qian, J., Thomson, A. F., Wu, Y., Weber, K. J. & Blakers, A. W. Impact of Perovskite/Silicon Tandem Module Design on Hot-Spot Temperature. *ACS Applied Energy Materials* **1**, 3025–3029

(2018).
63. Bowring, A. R., Bertoluzzi, L., O'Regan, B. C. & McGehee, M. D. Reverse Bias Behavior of Halide Perovskite Solar Cells. *Advanced Energy Materials* **8**, 1702365 (2017).
64. Ramaprabha, R. & Mathur, B. L. A comprehensive review and analysis of solar photovoltaic array configurations under partial shaded conditions. *International Journal of Photoenergy* **2012**, (2012).
65. Faÿ, S. & Shah, A. Zinc Oxide Grown by CVD Process as Transparent Contact for Thin Film Solar Cell Applications. in *Transparent Conductive Zinc Oxide: Basics and Applications in Thin Film Solar Cells* (eds. Ellmer, K., Klein, A. & Rech, B.) 235–302 (Springer, 2008).
66. Yang, J., Siempelkamp, B. D., Mosconi, E., de Angelis, F. & Kelly, T. L. Origin of the Thermal Instability in CH3NH3PbI3 Thin Films Deposited on ZnO. *Chemistry of Materials* **27**, 4229–4236 (2015).
67. Rolston, N. *et al.* Engineering Stress in Perovskite Solar Cells to Improve Stability. *Advanced Energy Materials* **8**, 1802139 (2018).
68. Schutt, K. *et al.* Overcoming Zinc Oxide Interface Instability with a Methylammonium-Free Perovskite for High-Performance Solar Cells. *Advanced Functional Materials* **29**, 1–8 (2019).
69. Lin, Y. *et al.* Dual-Layer Nanostructured Flexible Thin-Film Amorphous Silicon Solar Cells with Enhanced Light Harvesting and Photoelectric Conversion Efficiency. *ACS Applied Materials and Interfaces* **8**, 10929–10936 (2016).
70. Tsao, Y. C. *et al.* Rapid fabrication and trimming of nanostructured backside reflectors for enhanced optical absorption in a-Si:H solar cells. *Applied Physics A: Materials Science and Processing* **120**, 417–425 (2015).
71. Werner, J. *et al.* Improving Low-Bandgap Tin–Lead Perovskite Solar Cells via Contact Engineering and Gas Quench Processing. *ACS Energy Letters* **5**, 1215–1223 (2020).
72. Boyd, C. C. *et al.* Overcoming redox reactions at perovskite / nickel oxide interfaces to boost voltages in perovskite solar cells. *Joule* **4**, 1-17 (2020).
73. Boyd, C. C. *et al.* Barrier Design to Prevent Metal-Induced Degradation and Improve Thermal Stability in Perovskite Solar Cells. *ACS Energy Letters* **3**, 1772–1778 (2018).
74. Osterwald, C. R. Translation of device performance measurements to reference conditions. *Solar Cells* **18**, 269–279 (1986).
75. Meusel, M. *et al.* Spectral Response Measurements of Monolithic GaInP/Ga(In)As/Ge Triple-Junction Solar Cells: Measurement Artifacts and their Explanation. *Progress in Photovoltaics: Research and Applications* **11**, 499–514 (2003).